Engineering and Technology Journal
Journal homepage: https://etj.uotechnology.edu.iq

Fault Detection and Fault Tolerant Control for Anti-lock Braking Systems (ABS) Speed Sensors by Using Neural Networks

Ayad Q. Abdulkareem*, Abdulrahim Th. Humod, Oday A. Ahmed

Electrical Engineering Dept., University of Technology-Iraq, Alsina'a street, 10066 Baghdad, Iraq.
*Corresponding author Email: 30205@uotechnology.edu.iq

HIGHLIGHTS

- An active Fault Detection and Fault Tolerant Control FD-FTC method were implemented for the speed sensors fault utilized in the anti-lock braking system.
- Proposed Method FD-FTC is a Data-Based method implemented with a neural network model.
- The data required for training neural network models are obtained from the Quarter Car Model implemented with the MATLAB environment.
- During the applied test, the responses were accurate, and the implemented method served its design purpose.
- The proposed method will increase the reliability and safety of the anti-lock braking system used in modern vehicle braking systems.

ARTICLE INFO

Handling editor: Ivan A. Hashim

Keywords:
Anti-lock Braking System; Data Construction; Fault Tolerant Control; Neural Network, Residual Generation; Sensor Fault.

ABSTRACT

This paper proposed neural networks to continuously provide alternative constructed signals for vehicle and wheel speed sensors utilized for the Anti-Lock Braking System (ABS), which serves as the fault tolerant control method. These alternative constructed signals are used for two purposes. The first is to generate residual signals, and the second is to be adopted instead of isolated faulty signals. The residual signal is generated by extracting the difference between the alternative constructed signals and the corresponding actual signals. These residual signals serve as an indication of fault occurrence and to express that fault severity. Whenever a fault occurrence is detected and diagnosed in one of the sensor's signals, the faulty signal is isolated and replaced by the corresponding constructed signal to maintain the system's normal behavior under a faulty condition. The range of data covered under the proposed estimating neural networks is huge, continuous in time, and not sampled. In this work, the range of the data lies between [50 to 120 km/h] when the braking is started. That cannot be performed by any available method. These models' training process is based on the Levenberg-Marquardt (LM) algorithm, implemented and tested by MATLAB/Simulink. The results show that these models can accurately map the measured data into the desired output through the best-fit functions. The fast response of the trained models makes them suitable for real-time alternative signals for fault-tolerant purposes for speed sensors during hard or panic braking.

1. Introduction

Recently, the field of automotive technology has witnessed great development, especially with regard to vehicle stability and passenger safety. Therefore, it is important to include several safety systems that work to prevent drivers from having injuries while driving or during sudden braking [1]. Under full braking, especially sudden or panic braking, a large braking force will be applied to the brake cylinder of the wheel and lead to a wheel lock-up state [2]. In a wheel lock-up state, the wheel may slip on its roadway, leading to a minimum amount of maneuverability. In other words, the driver will not be able to control the wheel direction [3]. Additionally, the braking distance increases and the probability of accidents becomes very high [4]. To solve such a problem, the designers of automotive technology systems worked to develop efficient vehicle braking systems. They developed a functionally good, controllable braking system by incorporating several components, including electric, electronic, mechanical, and hydraulic [5, 6].

http://doi.org/10.30684/etj.2022.135106.1259
Received 09 August 2022; Accepted 12 September 2022; Available online 16 October 2022
2412-0758/University of Technology-Iraq, Baghdad, Iraq

One of these advanced braking system technologies is the Anti-lock Braking System (ABS), which controls brake torque to avoid a wheel lock-up state during braking [7]. IDCD. Maia [8] describes ABS as an electronic-based control system designed to provide the ability to steer a vehicle during a fully braking moment to avoid the wheel lock-up state.

The main objective of ABS is to regulate the brake pressure applied to the wheel brake cylinder to obtain maximum friction force and maintain the vehicle's lateral stability. This will reduce the stopping distance and, at the same time, it will ensure that directional control is maintained [9]. However, a core control for ABS is the relative slip computation accuracy, which in turn mainly depends on the measurement of two-speed sensors. These are vehicle speed and wheel speed sensors [10]. Consequently, any malfunction or fault that occurs in one of them will directly affect their output signal and lead to incorrect calculation of relative slip and, in turn, result in the occurrence of safety accidents. Thus, it is necessary to construct a control system that can detect and accommodate these faults automatically with a specific precalculated level of errors. Such a control system is called a Fault Tolerant Control system (FTC).Recently, the topic of fault tolerance has attracted the interest of many researchers, such as Widjiantoro and Indriawati [11]. They suggested an FTC for both the sensor and actuator used in ABS. In their method, an estimation for the occurred fault is performed by utilizing proportional-integral (PI) observers with an extended form of state space equation followed by a compensation mechanism or reconfiguration mechanism that is used to replace the unhealthy signal with the estimated signal to compensate for the produced control signal. Simulation results show that the control system's response to the proposed algorithm yields an improved dynamic behavior than SMC without fault tolerant properties. Moreover, the system presents an inherent characteristic to deal with minor faults in the hydraulic unit. Muhammad Pinandhito et al. [12] also proposed an FTC detection and isolation method for the faults that may occur in the ABS speed sensors. In their method, an algorithm for calculating residual signals is utilized in fault detection. Then, an SMC utilizes this residual signal to produce a compensated control signal. According to the response test results after applying the bias and sensitivity faults, the system with the AFTC algorithm can completely overcome the sensor defect. Hui Sun et al. [13] suggested a model-based FTC, an observer-based method to detect faults that may occur in the speed sensor of an aircraft ABS. In their work, a Sliding Mode Observer (SMO) is introduced for fault detection and diagnosis. After fault detection, SMO works as a wheel speed estimator to provide a suitable replacement for the faulty measured signal. So, the control operation automatically changes from wheel speed sensor-based to senseless-based mode, so an observer-based FTC scheme is developed. When the wheel speed sensor is damaged, or there is an outside disturbance, the ABS maintains the observed state and remains stable. The results from the simulation demonstrate the effectiveness of the suggested approach against various sensor faults. Zahedi et al. [14] designed a bank of sliding mode observers that are utilized for sensor fault detection and isolation in an ABS. They demonstrated that using numerical simulations. They could successfully detect and isolate possible faults in the sensor. However, such a method is limited in fault detectability to the n-number of the utilized observer. Furthermore, no strategy for the detected fault accommodation has been presented. From the aforementioned review of the literature on diagnosing ABS faults, all of them have used model-based methods for ABS fault detection and health monitoring. However, the analyzing process of fault detectability in the above illustrated methods is not concise. Also, the steps for implementing the FDI system for residual signal generation are not clear.

Additionally, Guo et al. [15] proposed a Sliding Mode Controller to keep the optimal slip for the ABS used in electric vehicles. A performance comparison was presented for the ABS bang-bang controller with and without the proposed SMC. With the SMC controller, there was an improvement in passenger comfort and brake stability. Also, the slip was more accurate with the increase in braking torque of the motor. However, in their work, no Active-FTC has not been employed to accommodate the malfunction or fault in actuators or both sensors. Finally, Cabasino et al. [16] presented fault diagnosis analysis using a petri net. The effectiveness of their method was confirmed by diagnosing specific cases. However, they did not rely on a mathematical model of the ABS in developing their methodology based on logical thinking. Also, they did not address the issues with fault isolation and detection. These points are different from the work presented in this paper.

In this work, a data-based active FDI and FTC method have been implemented to detect, isolate, and accommodate the faults that may occur in one of the ABS speed sensors. It works to generate an alternative constructed signal. They are used for two purposes. The first is to generate residual signals, and the second is to be adopted instead of isolated faulty signals. The residual signal is generated by extracting the difference between the alternative constructed signals and the corresponding actual signals. These residual signals serve as an indication of fault occurrence and to express that fault severity. Whenever a fault occurrence is detected and diagnosed in one of the sensor’s signals, the faulty signal is isolated and replaced by the corresponding constructed signal to maintain the system's normal behavior under a faulty condition. This suggested approach is implemented using the principle of fast processing Curve Fitting (CF) executed by Neural Networks (NNs). NNs have been employed in various fields due to, in part, a new powerful algorithm development that affects their ability to process information rapidly and leads to faster response [17- 20]. NNs provide a perfect tool with high accuracy and fast response solution for nonlinear CF problems [15]. Typically, the algorithms of NN are considerably faster than traditional iterative CF methods. Also, no initial guess is needed for the solution. Additionally, for real-time applications, there is an ability to implement the designed network model with special-purpose hardware, thereby exploiting the full capabilities of NN, including high processing speed.In the sequel, section ii presents background and related work. Next, section iii describes the proposed FT approach. Then, section IV provides the discussion of the results, and finally, the conclusion is presented in section V.

2. Research Methodology

2.1 Quarter Car Model

The Quarter Car Model (QCM) method is considered efficient for driving the ABS model. The QCM vehicle dynamics during braking are depicted in Figure 1 below [21].

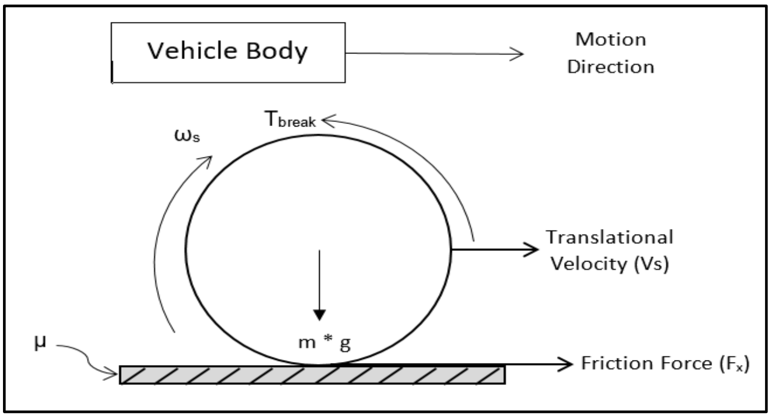

Figure 1: QCM model

That may be described according to the following equation:

$$F_x = \mathrm{m} \times g \times \mu(\lambda) \tag{1}$$

$$\dot{\omega} = (R \times F_x - T_b) \,/\, \mathrm{I} \tag{2}$$

$$\dot{V} = -F_x \div m \tag{3}$$

Then the longitudinal wheel slip (LWS) symbolized by λ may be calculated by:

$$\lambda = 1 - \frac{\omega R}{V} \tag{4}$$

Where I represents the moment of inertia of the wheel, represents wheel speed change ratio, R is the wheel radius, is the road-tire contact force, represents the braking torque, m represents the vehicle quarter mass, vehicle speed change ratio, g is the gravitational acceleration constant, and finally, μ is the Road Friction Coefficient (RFC). The calculation of RFC is performed based on a nonlinear relationship between itself and the LWS. This relationship is complex and depends on several parameters, such as tire state, speed of the vehicle, and road type[21]. Figure 2 shows RFC as a function of LWS for various road conditions.

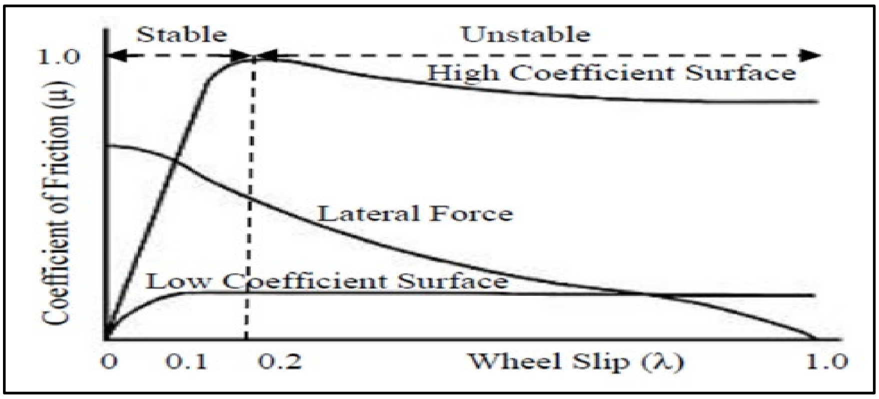

Figure 2: RFC (μ) versus LWS (λ)[21]

From Figure 2, the maximum braking force value can be achieved at LWS near 0.2 value for most road types. In other words, the ABS has to manipulate the braking torque to have the required LWS that results in efficient braking.

2.2 Fast Curve Fitting Using Neural Network

Curve fitting is a common problem in data analysis. It is the process of fitting parametrized functional forms to sets of empirical data [22]. The question is how to find the best values of these parameters. The best parameter values are typically determined by minimizing an error measure. This error measure is frequently assumed to be the sum of the squares of the errors between the actual data values and the predicted values by the function. Suppose the form of the function is linear or the function is linearly dependent on the parameter. In that case, the minimization problem is considered linear and can be solved easily. However, in many cases, it is important to consider that the functional forms depend nonlinearly on the parameters. In these situations, the error measure minimization process typically includes an iterative method that starts with initial guessed values. These iterative techniques require intensive computing ability and are hence slow. Furthermore, suitable initial parameter guessing may require human involvement to guarantee convergence to the desired solution for complicated problems. Therefore, there is great interest in techniques that perform fast and can automate fitting processes, especially for real-time applications or applications with high data volumes.

A neural network offers a novel technique to determine the optimal values of the function parameters. The algorithms of NN are typically much faster than those of conventional iterative CF techniques. Additionally, the solution does not require an initial guess, and there is an ability to implement the designed network model with special-purpose hardware and, in this way, take advantage of the full ability of NN, including high processing speed [17-20].

A Multi-Layer Perceptron (MLP) is the most commonly used network type. An MLP consists of nodes that are also called neurons or network units, as illustrated in Figure 3. In the diagram, each unit is represented by a circle, and the lines that connect them are referred to as weights or links. The network can be described as an analytical mapping between a set of input variables $x_m(m = 1, \dots, M)$ and a set of output variables $y_n(n = 1, \dots, N)$ the output equation is given by:

$$y_n(x_1, x_2 \dots . x_M) = \sum_{l=1}^{L} \widehat{\omega}_{nl} \, f\left(\sum_{m=1}^{M} \omega_{lm} \, x_m + \theta_l\right) + \widehat{\theta}_n \qquad (5)$$

Where ω is link weight, θ an offset value, and f(.) is a nonlinear transformation function called an activation function[23].

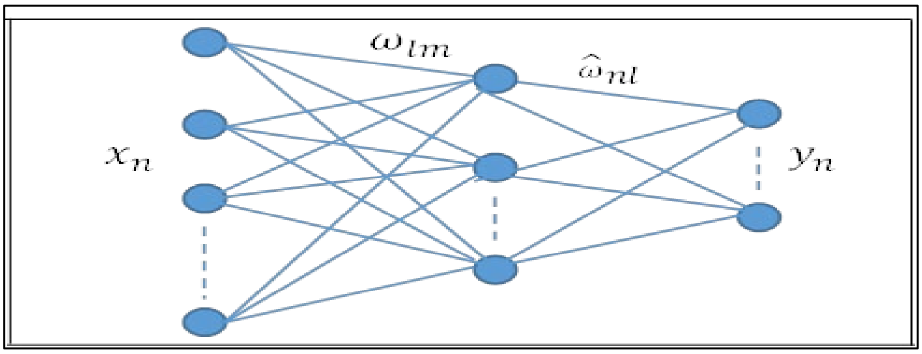

Figure 3: RFC (μ) versus LWS (λ)[21]

3. ABS Modelling and Data Collecting

Based on the QCM described in section 2.1, a MATLAB Simulink model for an ABS has been implemented, as shown in Figure 4. This model is used to collect the required data to serve as training data.

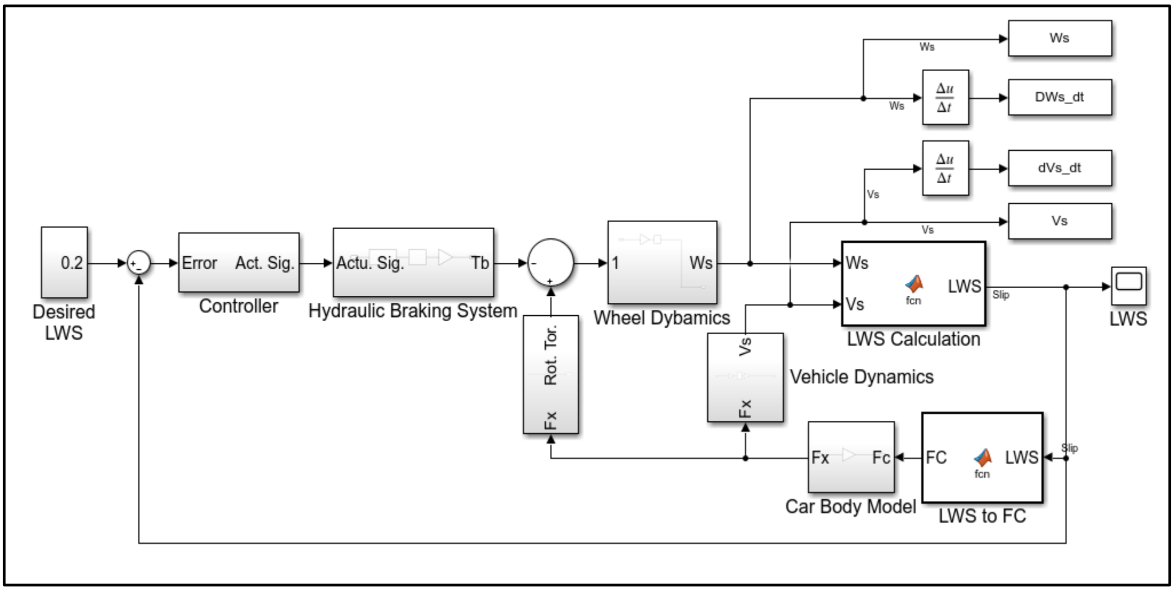

Figure 4: ABS Model Block Diagram

In this work, the road condition is assumed to be dry asphalt, the controller applied controller is a Bang-bang controller, the desired LWS is 0.2, and the remaining required ABS parameters are listed below in Table 1. The maximum speed is limited to 130 km/h, and various initial speeds have been applied below this maximum value. At each applied speed, four variables are observed, the vehicle speed data (V_s), the vehicle speed change ratio (dV_s/dt), the wheel speed data (ω_s), and the wheel speed change ratio ($d\omega_s/dt$). Then, two separate tables have applied an extraction and suitable arrangement for signal data. Each of these tables contains a total of 17,436 data samples. Each of these tables will serve as a database for the training objective for the corresponding neural model using the first and second models. A selected portion of these data samples is illustrated in Table 2 and Table 3 below.

Table 1: QCM Parameters utilized in the simulations

Symbol	Value
J	1.7 Kg-m2
R	0.326 meter
m	375 Kg
Initial Tb	0.01 Nm
Maximum Tb	1500 Nm
g	1.7 Kg-m2

Table 2: Training database for the first model (Randomly selected portion)

ω_s	$d\omega_s/dt$	V_s
45.8286	-45.0901	49.8547
45.4716	-35.7006	49.8114
45.1884	-28.3241	49.7652
44.96	-22.8395	49.7169
44.7706	-18.9334	49.6668
44.6071	-16.3515	49.6155

Table 3: Training database for second model (Randomly selected portion)

V_s	dV_s/dt	ω_s
46.8467	-6.3395	38.6199
46.7832	-6.3441	38.5126
46.7197	-6.3486	38.4072
46.6562	-6.3529	38.3037
46.5926	-6.3571	38.202
46.529	-6.3611	38.102

4. Data Constructing Models and Training Results

MLP networks have been built and trained in two separate but identical in topology. As shown in Figure 5 below, each model consists of an input layer, a hidden layer, and an output layer:

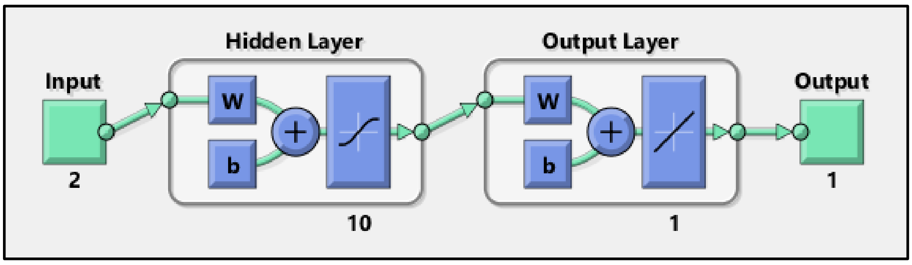

Figure 5: NN-MLP Based WSC Model Topology

Both MLP-NN models were evaluated using MATLAB (R2020a version), and these two models are Wheel Speed Constructor (WSC) models and used to construct wheel speed data. Its input layer is formed by the vehicle speed data (V_s) and vehicle speed change ration (dV_s/dt) while the output layer is formed by the wheel speed data (V_s) as shown in Figure 6.

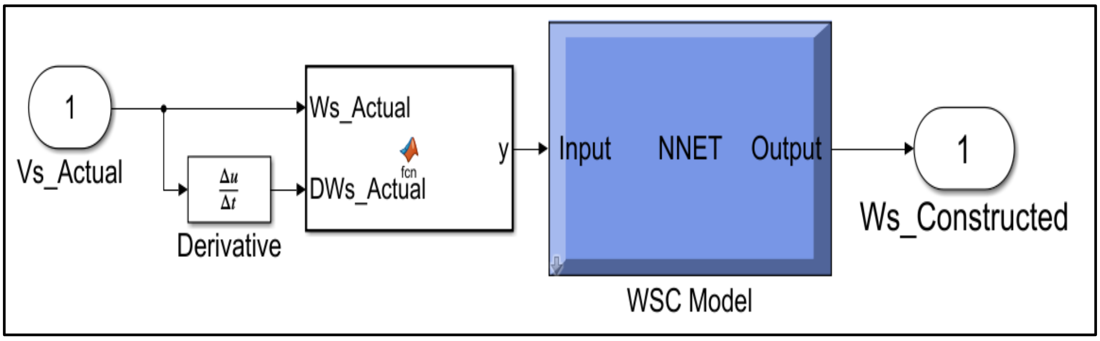

Figure 6: WSC Data Constructor model

The second is the Vehicle Speed Constructor (VSC) model used to construct vehicle speed data. Its input layer is formed by the wheel speed data (ω_s) and wheel speed change ration ($d\omega_s/dt$). While its output layer is formed by the vehicle speed data (V_s). As shown in Figure 7.

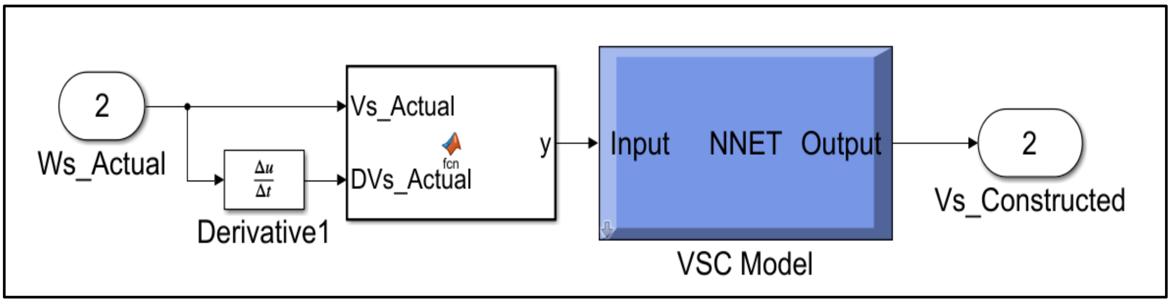

Figure 7: VSC Data Constructor model

The training process is performed based on the Levenberg-Marquardt (LM) training function, which is a feed-forward back-propagation network. It utilizes the separate datasets prepared in the previews section, one for the WSC model training and one for the VSC model training. As mentioned in the previews section, each of these data sets contains a total of 17,436 data samples. Each data set is further subdivided into three groups as follows: The first group is 70% (12206 samples) of the overall data set and is utilized for model training. These are known as the data sets from which the error is used to fit and adjust the network during training. The second group is 15% (2615 samples) of the overall data set and is utilized for validation. These datasets are known as the data used to measure how the trained network is general for real data checks and to stop training based on generalization results. The third group is 15% (2615 samples) of the overall data set and is utilized for testing purposes only. These datasets measure network performance independently after being trained and validated. Therefore, testing samples do not affect training datasets.

During training, the training data samples are set to the network, and the values of both biases and weights keep changing until the error of training data samples approaches the minimum acceptable limit.

Tables 4 and 5 illustrate the performance results for the two WSC and VSC-developed models, respectively. Both tables contain the values of the regression coefficient R2 and mean squared error MSE related to the three utilized datasets (training, testing, and validation datasets). It can be concluded that both trained models have very good performance as the MSE approaches zero and R2 closes to unity.

Table 4: Training Performance results of the VSC model

Data Sets	NO. of Samples	MSE	R2
Training	12206	6.71313e-1	0.999751
Validation	2615	6.36787e-1	0.999759
Testing	2615	1.12486e-0	0.999586

Table 5: Training Performance results of the VSC model

Data Sets	NO. of Samples	MSE	R2
Training	12206	1.90927e-1	0.999894
Validation	2615	2.35444e-1	0.999874
Testing	2615	2.01139e-1	0.999880

Figure 8 depicts the histogram plots used to predict the accuracy of the two presented models. From Figure8-a, it can be observed that the errors of the VSC developed models' output are mostly equal to zero or close to zero in the range of -1.861 to 2.272, where most of the output errors are equal to 0.4331, which is an indication of very good prediction performance from the developed model. From Figure8-b, it may also be observed that the error of the WSC developed models' output is mostly equal to zero or close to zero in the range of -1.334 to 0.7273. In addition, most of the output errors are equal to 0.04008, indicating very good prediction performance from the developed model.

Figure 9 illustrates, for the developed models, the variation of MSE for data of validation, testing, and training against the number of iterations. At the start of the iteration, both biases and weights continue to adjust, and the validation improves, reaching an optimal convergence limit.

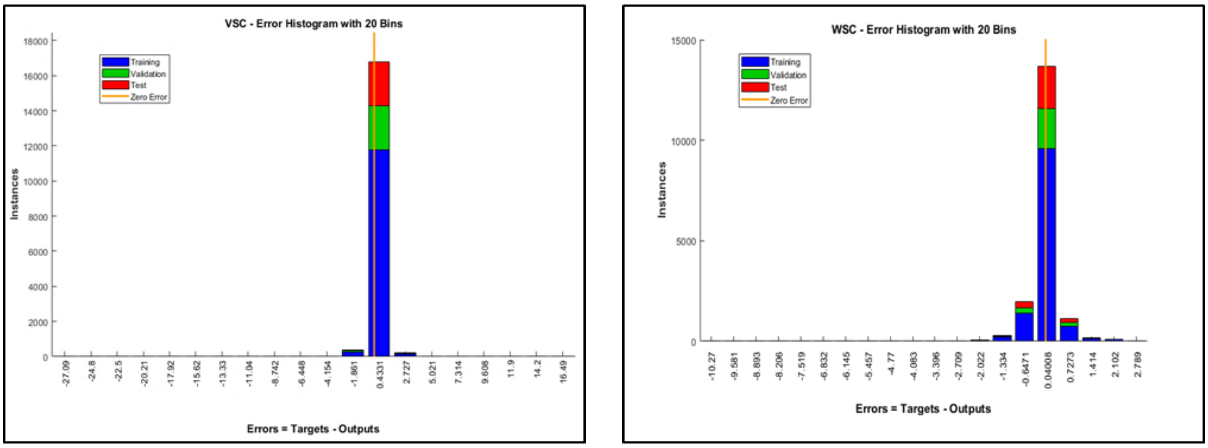

(a) (b)

Figure 8: Error Histogram for both developed models: (a) VSC model (b) WSC model

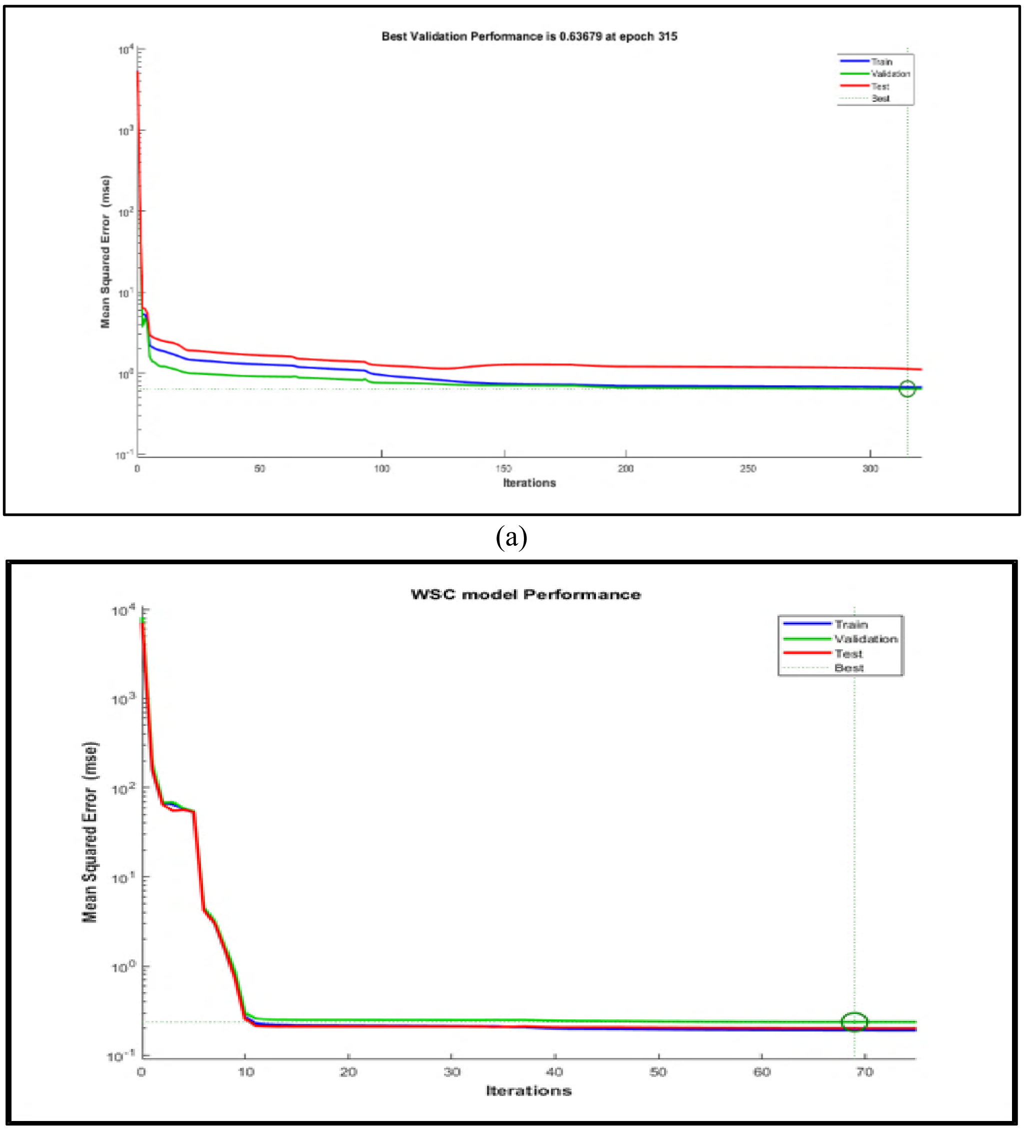

(a)

(b)

Figure 9: MSE variation with iteration for both developed models: (a): VSC model, (b) WSC model

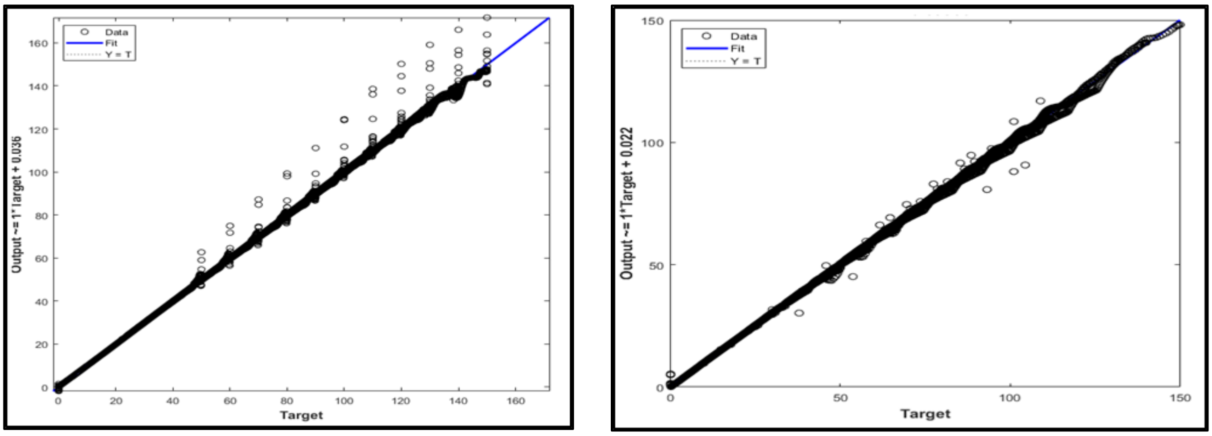

(a) (b)

Figure 10: MSE variation with iteration for both developed models: (a): VSC model, (b) WSC model

5. Data Construction Models Online Testing Results

After training is completed, the data construction unit is built and connected to the ABS model for an online test. As illustrated in Figure (11-a), the data construction unit contains the two trained models, the WSC and VSC models. The WSC receives the vehicle speed sensor signal as an input and utilizes it to construct an estimated signal equivalent to the wheel speed sensor signal. On the other hand, the VSC receives the wheel speed sensor signal as an input and utilizes it to construct an estimated signal equivalent to the vehicle speed sensor signal. Figure (11-b) shows the connection of the data construction unit to the ABS model.

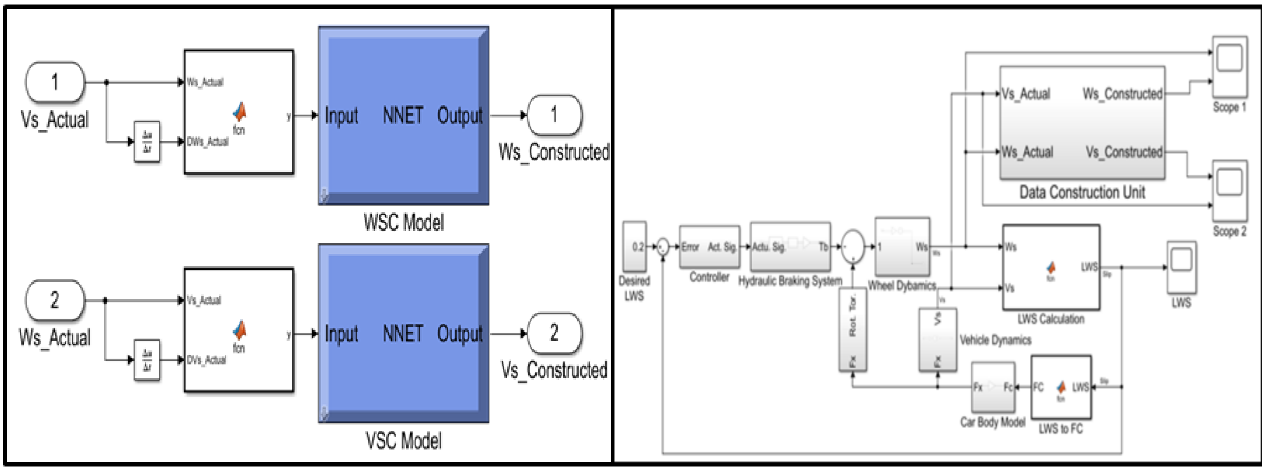

(a) (b)

Figure 11: Implemented System for Online Testing. (a): Data Construction Unit (b): ABS model with Data ConstructionUnit

5.1 System Test With Faultless Sensor Signal

According to the training results in section 2.3, each of the implemented data construction models can construct an accurate speed signal by utilizing the signal from the second sensor. To confirm such an ability, an online fault-free test has been applied. The applied test includes three different selected speeds. These selected speeds are 60, 80, and 100 km/h.

At each selected speed test, four signals are obtained: actual wheel speed sensor signal (Ws_actual), actual vehicle speed sensor signal (Vs_actual), constructed vehicle speed signal (Vs_Constructed), and constructed wheel speed signal (Ws_Constructed). Figures 12-a and 12-f illustrate the plot of these obtained signals at the three selected values: 60, 80, and 100 km/h, respectively. Where the two constructed speed signals (Vs_Constructed) and (Ws_Constructed) are compared to the corresponding actual speed signals (Vs_actual) and (Ws_actual), respectively. It can be seen that, despite the decrease in actual speed due to the braking process, there is a perfect match between the constructed signals and the corresponding actual signals.

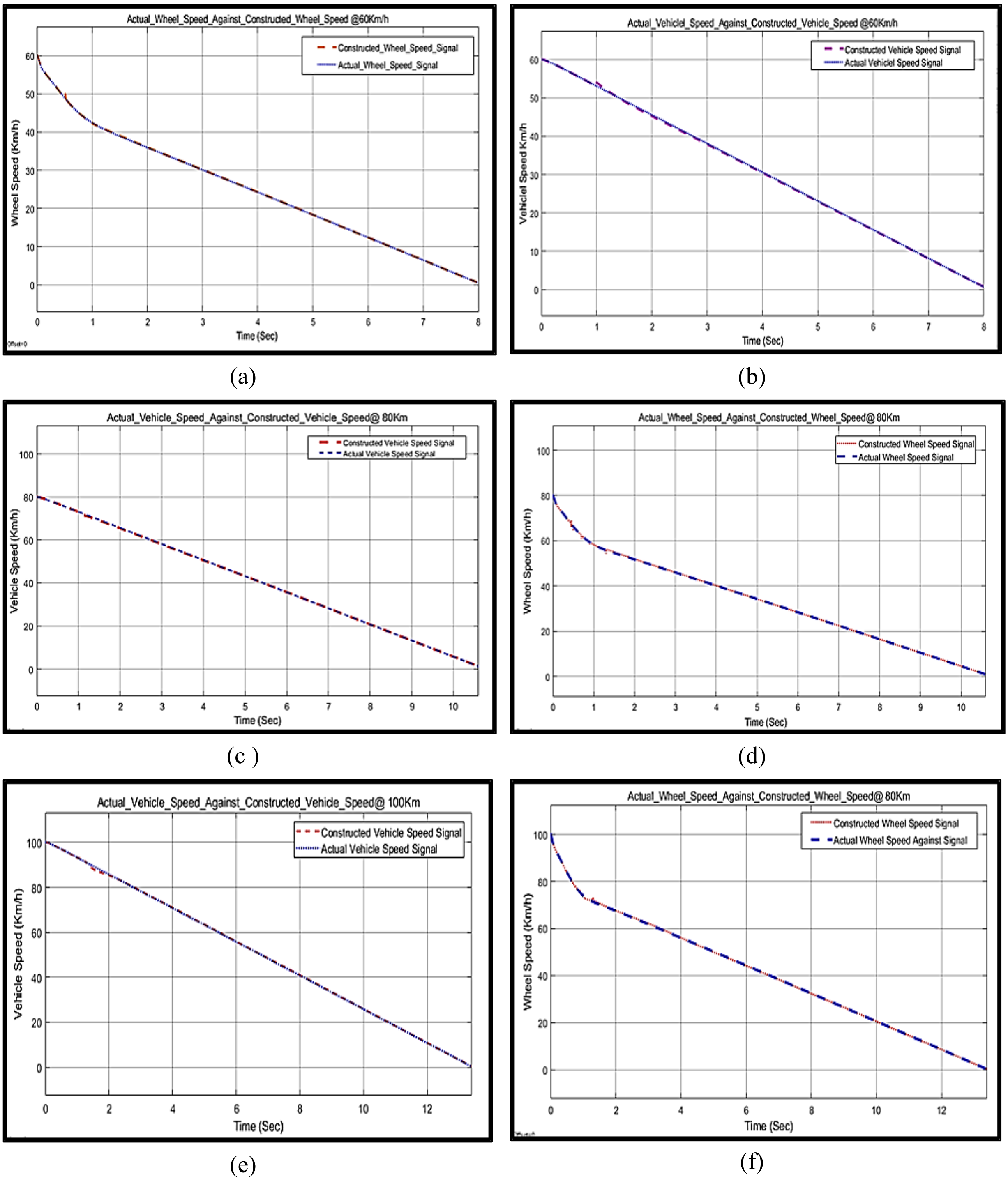

(a) (b)

(c) (d)

(e) (f)

Figure 12: Constructed data signals versus actual signals at three different speeds: (a) and (b) at 60 km/hr, (c) and (d) at 80 km/hr, and finally (e) and (f) at 100 km/hr

5.2 System Test with Defective Sensor Signal

A test has been applied under special operating conditions to express the proposed system's ability to detect and diagnose the sensor fault accurately. In these operating conditions, a fault signal F (t) is injected into one of the two sensors' signals. The Equation of the injected fault can be constructed as:

$$F(t) = \begin{cases} 10t - 40 & 4 \leq t \ \leq 5 \\ 60 - 10t & 5 \leq t \ \leq 6 \end{cases} \tag{6}$$

Figure (13) shows the injected fault signal $F(t)$.

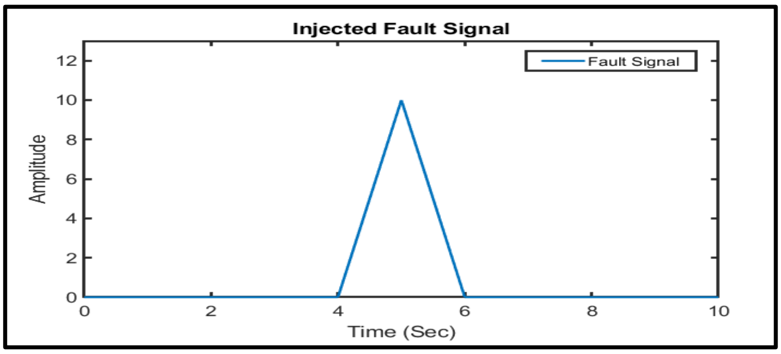

Figure 13: The proposed injected fault signal $F(t)$ related to equation (5)

The fault signal $\boldsymbol{F(t)}$ is injected into one of the speed sensors' signals. This injection operation is performed through a fault injection unit, as shown in Figure 14:

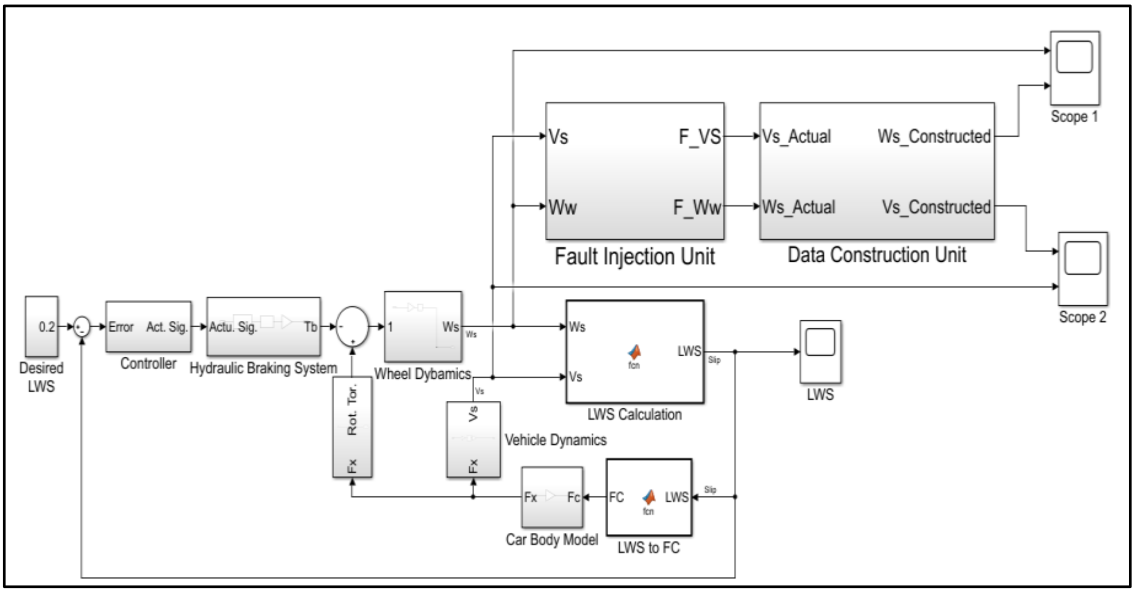

Figure 14: ABS model with Data Construction Unit and Fault Injection Unit

The fault injection unit works to add the proposed fault signal $F(t)$ to the actual healthy signal Vs or Ww and generate a corresponding faulty signal F_Vs or F_Ww, respectively.

During the applied test, the initial velocity is set to 70 km/h, and a fault signal is injected into the vehicle speed sensor. The response of the proposed system is expressed as shown in Figure (15-a). The figure shows that the faulty actual signal, Vs_Actual_Fault, is represented by a red-dash line. This signal is evaluated in a healthy state at times before 4 s and, after that, a faulty state. As can be seen, the fault of the vehicle speed sensor starts at 4 s and ends at 6 s, then the vehicle sensor returns to nominal behavior. Meanwhile, the corresponding constructed signal, Vs_Constructed, represented by a blue dashed line, displays the speed value without any flaw. Especially in between the 4s and 6s. Moreover, a residual signal results when a subtraction operation is performed between these two signals. This residual signal is shown in Figure (15-b).

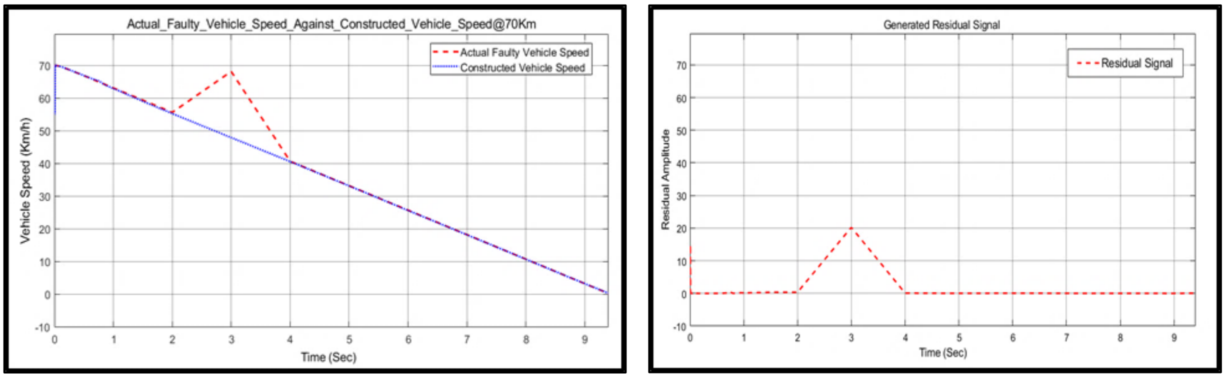

(a) (b)

Figure 15: Injected Fault Test Results: (a) Faulty vs. Constructed Signals and (b) Generated residual signal

The online testing results reflect the performance training results expressed in tables 4 and 5. The implemented proposed models fulfill their purpose where, under faulty free conditions, the constructed signals are accurate, and there is no phase shaft relative to the corresponding actual signals. This qualifies them as replacements for actual sensor signals whenever they cannot read them for any reason.

The same behavior is reflected under a faulty condition state. The generated residual signal accurately describes the drift in the actual signal due to fault occurrences and matches the injected fault signal in Figure 15. This will provide a precise indication of the severity of the occurrence and allow for appropriate fault management to be implemented.

Thus, the proposed system not only works to detect and diagnose the faulty signal that may occur in the ABS speed sensors. It also works to tolerate this fault by providing a healthy, constructed signal to substitute for that faulty signal. This will ensure safe vehicle braking under faulty conditions.

6. Conclusion

In this work, an FTC method was implemented for ABS speed sensors. First, data constructor models that utilize a NN based on MLP were implemented to achieve an accurate and fast response under a faulty state. These models work to provide an alternative, reliable signals for both ABS speed sensors. After preparing the datasets required for training each proposed model, a MATLAB (2020 version) environment is used for training and testing objectives. Then, performance evaluation for trained models under faulty and faulty-free states. Their responses were accurate, and the implemented method served its design purpose, especially under a faulty state.

Although all the preview benefits, there is a specific condition that arises when a fault occurs, which is, when one of the sensors is faulty, according to the proposed method, it will be detected by the residual signal, and a fault occurrence will be declared. But, at the same time, this faulty signal is currently being used to construct a corresponding signal for the other sensor, which will clearly result in an inaccurate constructed signal, leading to a false fault occurrence. Therefore, to overcome such an issue, an additional method needs to be applied that works simultaneously to isolate the faulty signal from being used by its related data constructor to avoid a false fault detection alert. This problem needs to be solved.

Acknowledgment

The authors would like to acknowledge the electrical engineering department, University of Technology- Iraq, for their guidance and support throughout this study.

Author Contribution

All authors contributed equally to this work.

Funding

No external funding was received for this research.

Data Availability Statement

The data that support the findings of this study are available on request from the corresponding author.

Conflicts of Interest

Authors declare that their present work has no conflict of interest with other published works.

References

[1] Y. Huang and Y. Chen, Vehicle Lateral Stability Control Based on Shiftable Stability Regions and Dynamic Margins, IEEE Trans. Veh. Technol., 69 (2020) 14727–14738. https://doi.org/10.1109/TVT.2020.3036780

[2] D. Savitski et al., Wheel Slip Control for the Electric Vehicle with In-Wheel Motors: Variable Structure and Sliding Mode Methods, IEEE Trans. Ind. Electron., 67 (2020) 8535–8544. https://doi.org/10.1109/TIE.2019.2942537

[3] L. Yuan, H. Chen, B. Ren, and H. Zhao, Model predictive slip control for electric vehicle with four in-wheel motors. Chinese Control Conf. CCC, 2015,2015,. 7895–7900. https://doi.org/10.1109/ChiCC.2015.7260894

[4] G. Cui, J. Dou, S. Li, X. Zhao, X. Lu, and Z. Yu, Slip Control of Electric Vehicle Based on Tire-Road Friction Coefficient Estimation, Math. Probl. Eng., 2017, 2017. https://doi.org/10.1155/2017/3035124

[5] M. L. H. Muhammad Luqman, K. Hudha, F. Ahmad, and H. Jamaluddin, Design and clamping force modelling of electronic wedge brake system for automotive application, Int. J. Veh. Syst. Model. Test., 8 (2013) 145–156. https://doi.org/10.1504/IJVSMT.2013.054478

[6] F. Bin Ahmad, K. Hudha, and H. Jamaluddin, Gain scheduling PID control with pitch moment rejection for reducing vehicle dive and squat, Int. J. Veh. Saf., 4 (2009) 45–83. https://doi.org/10.1504/IJVS.2009.026973

[7] W. Zhang ,X. Guo, An ABS control strategy for commercial vehicle,IEEE/ASME Trans. Mechatronics, 20 (2015) 384–392. https://doi.org/10.1109/TMECH.2014.2322629

[8] I. D. De Carvalho Dantas Maia, Modeling and control of anti-lock braking systems considering different representations for tire-road interaction, 23rd Int. Conf. Syst. Theory, Control Comput. ICSTCC 2019 - Proc., 2019. https://doi.org/10.1109/ICSTCC.2019.8885694

[9] A. A. Aly, E.-S. Zeidan, A. Hamed, F. Salem, An Antilock-Braking Systems (ABS) Control: A Technical Review. Intell. Control Autom., 02 (2011) 186–195. https://doi.org/10.4236/ica.2011.23023

[10] Y. Yang, Q. Tang, L. Bolin, C. Fu, Dynamic coordinated control for regenerative braking system and anti-lock braking system for electrified vehicles under emergency braking conditions, IEEE Access, 8 (2020) 172664–172677. https://doi.org/10.1109/ACCESS.2020.3024918

[11] B. L. Widjiantoro and K. Indriawati, Sensor/actuator fault tolerant sliding mode control for anti-lock braking in a quarter electric vehicle, Int. J. Power Electron. Drive Syst., 11 (2020) 1220–1229. https://doi.org/10.11591/ijpeds.v11.i3.pp1220-1229

[12] M. R. Pinandhito, K. Indriawati, and M. Harly, Active fault tolerant control design in regenerative antilock braking system of electric vehicle with sensor fault, AIP Conf. Proc., 2088, 2019. https://doi.org/10.1063/1.5095276

[13] H. Sun, J. Yan, Y. Qu, and J. Ren, Sensor fault-tolerant observer applied in UAV anti-skid braking control under control input constraint, J. Syst. Eng. Electron., 28 (2017) 126–136. https://doi.org/10.21629/JSEE.2017.01.14

[14] E. Zahedi and A. A. Gharaveisi, Fault detection and isolation of Anti-lock Braking System sensors, Proc. - 2011 2nd Int. Conf. Control. Instrum. Autom. ICCIA 2011, 7 (2011) 258–263. https://doi.org/10.1109/ICCIAutom.2011.6356666

[15] J. Guo, X. Jian, G. Lin, Performance evaluation of an anti-lock braking system for electric vehicles with a fuzzy sliding mode controller, Energies, 7 (2014) 6459–6476. https://doi.org/10.3390/en7106459

[16] M. P. Cabasino, A. Giua, C. Seatzu, A. Solinas, and K. Zedda, Fault diagnosis of an ABS system using Petri nets, IEEE Int. Conf. Autom. Sci. Eng., 2011,594–599. https://doi.org/10.1109/CASE.2011.6042508

[17] O. I. Abiodun, A. Jantan, A. E. Omolara, K. V. Dada, N. A. E. Mohamed, and H. Arshad, State-of-the-art in artificial neural network applications: A survey, Heliyon, 2018. https://doi.org/10.1016/j.heliyon.2018.e00938

[18] A. Abed, S. Gitaffa, A. Issa, Quadratic Support Vector Machine and K-Nearest Neighbor Based Robust Sensor Fault Detection and Isolation, Eng. Technol. J., 39 (2021) 859–869. https://doi.org/10.30684/etj.v39i5a.2002

[19] N. T. Mahmooda, M. H. Al-Muifraje, S. K. Salih, T. R. Saeed, Pattern Recognition of Composite Motions based on EMG Signal via Machine Learning, Eng. Technol. J., 39 (2021) 295–305. https://doi.org/10.30684/etj.v39i2a.1743

[20] S. Nasser, I. Hashim, W. Ali, Visual Depression Diagnosis From Face Based on Various Classification Algorithms, Eng. Technol. J., 38 (2020) 1717–1729. https://doi.org/10.30684/etj.v38i11a.1714

[21] O. Tur, O. Ustun, R. N. Tuncay, An introduction to regenerative braking of electric vehicles as anti-lock braking system, IEEE Intell. Veh. Symp. Proc., 2007. https://doi.org/10.1109/ivs.2007.4290238

[22] N. Pattanadech , P. Yutthagowith, Fast curve fitting algorithm for parameter evaluation in lightning impulse test technique,IEEE Trans. Dielectr. Electr. Insul., 22 (2015) 2931–2936. https://doi.org/10.1109/TDEI.2015.005165

[23] M. T. Hagan, H. B. Demuth, and O. De Jesús, An introduction to the use of neural networks in control systems, Int. J. Robust Nonlinear Control, 12 (2002) 959–985. https://doi.org/10.1002/rnc.727